

# Initial risk stratification and staging in prostate cancer with prostatic-specific membrane antigen positron emission tomography/computed tomography: A first-stop-shop

## ABSTRACT

Current imaging for prostate cancer (PCa) had limitations for risk stratification and staging. Magnetic resonance imaging frequently underestimated lymph node metastasis while bone scintigraphy often had diagnostic dilemmas. Prostatic-specific membrane antigen (PSMA) positron emission tomography-computed tomography (PET/CT) has been remarkable in PCa recurrence. Ninety-seven PSMA PET-CT scans were reanalyzed for tumor node metastases staging and risk stratification of lymph node and distant metastasis proportion. Histopathology of 23/97 patients was available as gold standard. Chi-square test was used for proportion comparison. Sensitivity, specificity, positive predictive value (PPV), negative predictive value (NPV), overestimation, underestimation, and correct estimation of T and N stages were calculated. Kappa coefficient ( $\kappa$ ) was derived for inter-rater agreement. Lymph node or distant metastasis detection on PSMA PET/CT increased significantly with increase in risk category. PSMA PET/CT sensitivity, specificity, PPV, and NPV for extraprostatic extension, seminal vesicle invasion, and lymph node metastases were 63.16%, 100%, 100%, 36.36%; 55%, 100%, 100%, 25%; and 65.62%, 99.31%, 87.50%, and 97.53%, respectively. Kappa coefficient showed substantial agreement between PSMA PET/CT and histopathological lymph node metastases ( $\kappa = 0.734$ ); however, it was just in fair agreement ( $\kappa = 0.277$ ) with T stage. PSMA PET/CT overestimated, underestimated, and correct estimated T and N stages in 8.71%, 39.13%, 52.17% and 8.71%, 4.35%, and 86.96% cases, respectively. PSMA PET/CT has potential for initial risk stratification with reasonable correct N stage estimation, however underestimates T stage. Hence, we concluded that PSMA PET/CT should be used as “first-stop-shop” for staging and initial risk stratification of PCa with regional magnetic resonance imaging in surgically resectable cases.

**Keywords:** Extrapelvic lymph node, first-stop-shop, initial risk stratification, prostatic-specific membrane antigen positron emission tomography-computed tomography, spleen, staging

## INTRODUCTION

Current imaging for prostate cancer (PCa) had limitations for risk stratification and staging. Magnetic resonance imaging (MRI) frequently underestimated lymph node metastasis<sup>[1]</sup> while bone scintigraphy (BS) often had diagnostic dilemmas.<sup>[2,3]</sup> Hence, various mathematical predictive models have been developed in time for risk stratification.<sup>[4-10]</sup> Glu-NH-CO-NH-Lys-(Axe)-[<sup>68</sup>Ga(HBED-CC)] <sup>68</sup>Ga-prostatic-specific membrane antigen positron emission tomography-computed tomography (<sup>68</sup>Ga-PSMA PET-CT) has shown promising results in suspected recurrent PCa.<sup>[11-14]</sup> Few

**MANOJ GUPTA, PARTHA SARATHI CHOUDHURY, SUDHIR RAWAL<sup>1</sup>, HARISH CHANDRA GOEL<sup>2</sup>, VINEET TALWAR<sup>3</sup>, AMITABH SINGH<sup>1</sup>, SAROJ KUMAR SAHOO**


Departments of Nuclear Medicine, <sup>1</sup>Uro-Gynae Surgical Oncology and <sup>3</sup>Medical Oncology, Rajiv Gandhi Cancer Institute and Research Centre, New Delhi, <sup>2</sup>Amity Centre for Radiation Biology, Amity University, Noida, Uttar Pradesh, India

**Address for correspondence:** Dr. Manoj Gupta, Department of Nuclear Medicine, Rajiv Gandhi Cancer Institute and Research Centre, Sector 5, Rohini, New Delhi - 110 085, India. E-mail: docmanojgupta@yahoo.com

This is an open access journal, and articles are distributed under the terms of the Creative Commons Attribution-NonCommercial-ShareAlike 4.0 License, which allows others to remix, tweak, and build upon the work non-commercially, as long as appropriate credit is given and the new creations are licensed under the identical terms.

**For reprints contact:** reprints@medknow.com

**How to cite this article:** Gupta M, Choudhury PS, Rawal S, Goel HC, Talwar V, Singh A, *et al.* Initial risk stratification and staging in prostate cancer with prostatic-specific membrane antigen positron emission tomography/computed tomography: A first-stop-shop. World J Nucl Med 2018;17:261-9.

Access this article online	
<b>Website:</b> www.wjnm.org	<b>Quick Response Code</b> 
<b>DOI:</b> 10.4103/wjnm.WJNM_79_17	

studies have suggested its role in lymph node staging and prognostication.<sup>[15-18]</sup> However, its role in risk stratification has not been addressed. We hypothesized that PSMA PET-CT has a potential to become first-stop-shop imaging for PCa staging workup.

## MATERIALS AND METHODS

From our database of <sup>68</sup>Ga-PSMA PET-CT studies from July 2014 to March 2017, we found 114 newly diagnosed PCa patients referred for initial staging. Patients' data were retrieved from computerized patient record system and picture archiving and communication system. Ninety-seven patients with adenocarcinoma prostate whose baseline prostate-specific antigen (PSA) and Gleason score were available were reanalyzed as per the American Joint Committee on Cancer 7<sup>th</sup> edition<sup>[19]</sup> criteria. Tumor, lymph node, metastasis (TNM) from PSMA PET-CT data was analyzed for risk stratification for lymph node and distant metastasis. We considered the following three risk categories: low (Gleason  $\leq 6$ , PSA  $\leq 10$   $\mu\text{g/L}$ , and T stage  $\leq \text{T2a}$ ), intermediate (Gleason 7, PSA  $> 10$ – $20$   $\mu\text{g/L}$ , and T stage  $\text{T2b}$ – $\text{T2c}$ ), and high (Gleason 8–10, PSA  $> 20$ , and T stage  $\geq \text{T3a}$ ). We further divided the risk categories into three groups based on single variable (PSA or Gleason or T stage) or dual variables (PSA + Gleason) or three variables (PSA + Gleason + T stage) which is the standard one.<sup>[20]</sup> For distant metastasis ( $M_1$ ), we further analyzed different substages ( $M_{1a}$ ,  $M_{1b}$ , and  $M_{1c}$ ) and type of bone metastasis (sclerotic, lytic, marrow, or mixed). Correlation between single voxel maximum standard uptake value ( $\text{SUV}_{\text{max}}$ ) of primary prostate, lymph node, and metastasis was also done. Histopathology of 23/97 (23.71%) patients who underwent radical prostatectomy with bilateral pelvic lymph node dissection (RP + BPLND) was taken as gold standard for T and N staging.  $\text{SUV}_{\text{max}}$  of prostate was correlated with PSA, Gleason score, pathological T stage, perineural invasion (PNI), lymphovascular invasion (LVI), extraprostatic extension (EPE), seminal vesicle invasion (SVI), and pathological lymph node status. Both focal and extensive extracapsular extension (ECE) and unilateral or bilateral SVI were taken as positive for involvement for statistical calculations.

Standard protocol for in-house synthesis of <sup>68</sup>Ga-PSMA and PET-CT acquisition was used.<sup>[21,22]</sup> PSMA-11 was acquired from advanced biochemical compounds (ABx) and labeling was done in IQS-fluidic labeling module (iTG) using 1.11 GBq iTG self-shielded Ga-68 generator. Two MBq/kg body weight of labeled PSMA-11 was injected intravenously, and a full body scan (vertex to mid thigh) was acquired with a dedicated full-ring hybrid PET-CT system (Biograph TruePoint40 with LSO crystal from Siemens Healthcare at Rajiv Gandhi Cancer

Institute and Research Centre, Delhi, India) with 4 min per bed position in three-dimensional mode. A low-dose CT scan (40 mAs and 120 kVp) was used for attenuation correction and anatomical localization.  $\text{SUV}_{\text{max}}$  normalized to body weight was recorded for prostate gland, lymph node, and bone metastasis.

### Image interpretation

All PSMA PET-CT studies were reinterpreted independently by two nuclear medicine physicians without knowledge of histopathology findings. Increased PSMA uptake in prostate and lymph node in comparison to background was taken as positive for involvement. No size criterion was used for lymph node interpretation. Visible irregular prostate outline or involvement of extraprostatic structure was taken as positive for EPE. Similarly, increased PSMA uptake more than the background in either or both seminal vesicles was considered positive for disease. Maximum value of  $\text{SUV}_{\text{max}}$  was recorded for both primary and metastatic sites.

### Statistical analysis

Chi-square test was used for lymph node and metastasis proportion comparison in various risk groups and *P* value was calculated. Spearman's rank test was used for the entire correlation. Sensitivity, specificity, positive predictive value (PPV), and negative predictive value (NPV) were calculated for T and N staging for PSMA PET-CT, considering histopathology as gold standard. Overestimation, underestimation, and correct estimation of T and N stage were calculated. Cohen's Kappa coefficient ( $\kappa$ ) was derived to see inter-rater agreement between PSMA PET-CT and histopathology for T and N stages. Uni- and multivariate regressions were done to find risk factors for lymph node metastasis using various clinical, imaging, and pathological parameters. *P* < 0.05 was considered statistically significant. IBM SPSS version 21 (IBM, New York, United States) was used for the entire statistical analysis.

## RESULTS

Patients' data (*n* = 97) were categorized based on various clinical risk variables and proportion for lymph node and distant metastasis in PSMA PET-CT. This is summarized in Table 1. Majority of patients were >50 years of age (94.85%), with age range of 38–88 years (median: 66 years) in our study. No significant difference was seen in the detection rate of lymph node and metastasis, with age as a risk factor. Detection of lymph node or distant metastasis increased with increase in risk category (*P* < 0.05) based on either single variable (Gleason or PSA) or when combining three variables (Gleason + PSA + T stage). Similar relationship was noticed with increase in T stage ( $\text{T}_{2a}$  to  $\text{T}_4$ ). Risk

**Table 1: Prostatic-specific membrane antigen positron emission tomography-computed tomography-based risk stratification for lymph node and distant metastasis proportion in various risk categories**

Risk categories	Number of patients (n=97)	Metastatic lymph node (N <sub>1</sub> ), n (%)	P	Distant metastasis (M <sub>1</sub> ), n (%)	P
Age (years)					
≤50	5	4 (80.00)	0.645	3 (60.00)	1.000
>50	92	55 (59.78)		49 (53.26)	
Gleason					
Low (≤6)	10	2 (20.00)	0.0002	1 (10.00)	0.004
Intermediate (7)	30	13 (43.33)		14 (46.67)	
High (8-10)	57	44 (77.19)		37 (64.91)	
PSA (µg/L)					
Low (≤10)	6	2 (33.33)	0.039	2 (33.33)	0.013
Intermediate (>10-20)	21	9 (42.86)		6 (28.57)	
High (>20)	70	48 (68.57)		44 (62.86)	
PSMA PET tumor stage					
T2a	2	0	<0.0001	0	<0.0001
T2b	9	2 (22.22)		0	
T2c	15	3 (20.00)		3 (20.00)	
T3a	11	9 (81.82)		8 (72.73)	
T3b	38	26 (68.42)		23 (60.53)	
T4	22	19 (86.36)		18 (81.82)	
Two variables (Gleason+PSA)					
Low (Gleason ≤6 + PSA ≤10)	1	0	0.069	0	0.182
Intermediate (Gleason 7 + PSA >10-20)	79	45 (56.96)		40 (50.63)	
High (Gleason 8-10 + PSA >20)	17	14 (82.35)		12 (70.59)	
Three variables (Gleason + PSA + PSMA tumor stage)					
Intermediate (Gleason 7 + PSA >10-20 + T2b-T2c)	59	25 (42.37)	<0.0001	22 (37.29)	0.0001
High (Gleason 8-10 + PSA >20 + ≥T3a)	38	34 (89.47)		30 (78.95)	

PSMA: Prostatic-specific membrane antigen; PET: Positron emission tomography; PSA: Prostate-specific antigen

categories based on two variables' (Gleason + PSA) group however showed near significant increase in the proportion of lymph node detection ( $P = 0.069$ ). Correlation of risk categories based on two variables with distant metastasis did not show statistically significant correlation ( $P = 0.182$ ). This was likely to be due to increased number of patients belonging to intermediate-risk category (81.44%) in this group.

On analyzing the 52/97 (53.61%) M<sub>1</sub> cases, we found 9 (17.31%), 35 (67.31%), and 8 (15.38%) patients belonging to M<sub>1a</sub> (extra-pelvic lymph node metastasis), M<sub>1b</sub> (bone ± lymph node metastasis), and M<sub>1c</sub> (other soft-tissue metastasis ± bone) categories, respectively. Besides retroperitoneal lymph nodes in nine M<sub>1a</sub> patients, three patients had inguinal and other three had mediastinal lymph nodal involvement as well. Considering the patients with bone metastasis (35/97), 24 (57.41%), 14 (33.33%), 3 (7.14%), and 1 (2.38%) had sclerotic, mixed, marrow, and lytic types of lesions, respectively. Further, we found 5 (11.90%), 6 (14.29%), and 31 (73.81%) patients with bone metastasis to have 1, 2–3, and >3 PSMA-positive bone lesions. Details of patients with solitary bone metastasis ( $n = 5$ ) are summarized in

Table 2. All these five patients belong to high-risk category without regional lymph nodal metastasis in three of them. Four patients had lesion in pelvic bones and one in the sternum [Figure 1].

All eight patients with M<sub>1c</sub> disease were in high-risk category and had lung ( $n = 5$ ), spleen, liver, and muscle as sites of involvement [Figure 2]. Seven of eight of these patients had associated bone metastasis and the remaining one patient with liver metastasis had T<sub>4</sub>N<sub>1</sub>M<sub>1a</sub> disease. For characterization of liver and splenic lesions, ultrasound correlation was performed which showed suspicious hypoechoic lesion. Pathological correlation was not done in these cases in view of other sites of already documented metastatic disease. Spearman's rank correlation of SUV<sub>max</sub> of prostate with highest SUV<sub>max</sub> in lymph nodes ( $r_s = 0.531$ ,  $P < 0.0001$ ) and distant metastatic lesions ( $r_s = 0.568$ ,  $P = 0.0001$ ) showed a positive correlation, meaning that similar intensity of receptor expression is expected in the primary as well as metastatic diseases.

The detailed analysis of 23 patients who underwent RP + BPLND following PSMA PET-CT is summarized in

**Table 2: Clinical and prostatic-specific membrane antigen positron emission tomography-computed tomography details of five patients with solitary bone metastasis**

	1	2	3	4	5
Age (years)	60	50	66	70	62
Gleason	4+4	4+4	4+3	3+4	3+4
PSA ( $\mu\text{g/L}$ )	20.1	22.4	21.1	27.3	17.3
PSMA tumor stage	T3a	T3b	T2c	T3b	T3b
Prostate SUV	5.3	9.7	6.1	6.9	14
N1/N0	N1	N0	N0	N0	N1
Node SUV	2.5	-	-	-	33.4
Site of bone metastasis	Right acetabulum	Right ischium	Right pubis	Left femur inter-trochanteric region	Sternum
Type of bone metastasis	Sclerotic	Sclerotic	Marrow	Sclerotic	Sclerotic
Bone lesion SUV	2.4	4	5.7	3.2	8.2

PSMA: Prostatic-specific membrane antigen; PSA: Prostate-specific antigen; SUV: Standardized uptake value

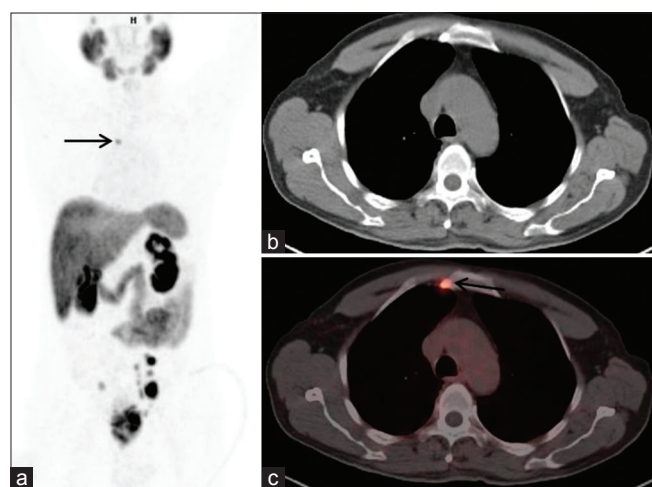


**Figure 1:**  $^{68}\text{Ga}$ -prostatic-specific membrane antigen positron emission tomography-computed tomography maximum intensity projection (a), axial computed tomography (b), and axial fused positron emission tomography-computed tomography (c) images showing prostatic-specific membrane antigen avid prostate lesion with pelvic lymph nodes and a solitary bony lesion in sternum (black arrow)

Table 3. The sensitivity, specificity, PPV, and NPV of PSMA PET-CT for detection of EPE and SVI were 63.16%, 100%, 100%, 36.36% and 55%, 100%, 100%, and 25%, respectively. Out of seven patients with false negative for EPE by PSMA PET-CT, four patients had focal microscopic invasion. Out of four patients with false-negative SVI by PSMA PET-CT, three patients had bilateral and one had unilateral invasion. A total of 469 lymph nodes (average: 20.4 per patient) were dissected in 23 patients. Positive histopathology was seen in 32 lymph nodes in nine patients. The sensitivity, specificity, PPV, and NPV of PSMA PET-CT per patient and per lymph node basis were 77.78%, 92.86%, 87.50%, 86.67% [Table 4] and 65.62%, 99.31%, 87.50%, and 97.53% [Table 5], respectively. Cohen's Kappa coefficient showed substantial agreement between PSMA PET-CT and histopathology-positive lymph node findings per patient ( $\kappa = 0.721$ ) and per lymph node ( $\kappa = 0.734$ ) basis. However, Cohen's Kappa coefficient showed just fair agreement ( $\kappa = 0.277$ ) between PSMA

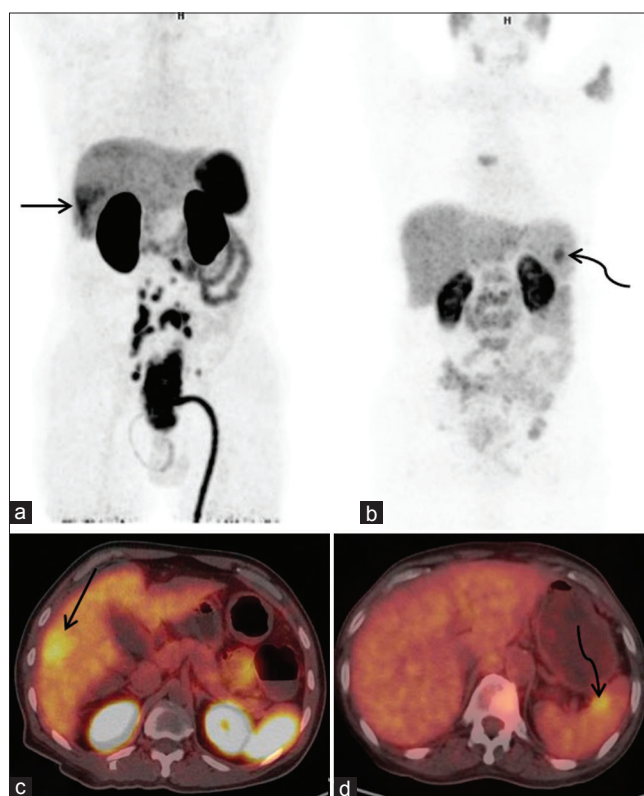


**Figure 2:**  $^{68}\text{Ga}$ -prostatic-specific membrane antigen positron emission tomography-computed tomography maximum intensity projection (a and b) and axial fused positron emission tomography-computed tomography (c and d) images showing prostatic-specific membrane antigen avid liver lesion (black arrow) and spleen lesion (black curved arrow)

PET-CT and histopathology T stage though the level of agreement was significant [Table 6]. The sensitivity, specificity, PPV, and NPV of PSMA PET-CT per lymph node basis for intermediate- and high-risk categories were 53.33%, 99.58%, 88.89%, 97.12% and 76.47%, 99.00%, 86.67%, and 98.02%, respectively. PSMA PET-CT overestimated, underestimated, and correct estimated T and N stages in 8.71%, 39.13%, 52.17% and 8.71%, 4.35%, and 86.96% cases, respectively. On univariate logistic regression for risk factors (age, PSA, Gleason score, T stage, PNI, LVI, EPE, SVI,

**Table 3: Clinical, prostatic-specific membrane antigen positron emission tomography-computed tomography and histopathological findings of 23 patients who underwent radical prostatectomy with bilateral pelvic lymph node dissection**

Age (years)	PSA (µg/L)	PSMA PET findings					Histopathology findings					Lymph node findings							
		EPE (no/yes/focal)	SVI (no/both/right/left)	Tumor stage	Prostate SUV	Lymph node Findings		EPE (no/yes/focal)	SVI (no/both/right/left)	Tumor stage	PNI	LVI	Gleason	Total sampled		Total positive		Nodal Stage	
						Nodal stage	Right							Left	Right	Left	Right		Left
76	8.7	No	No	T2a	11.2	N0	0	0	Focal	No	Yes	No	4+3	7	3	4	0	0	N0
65	24.4	No	No	T2c	10.1	N0	0	0	Focal	No	No	No	3+4	19	10	9	0	0	N0
63	18.8	Yes	Left	T3b	17.4	N0	0	0	Yes	Left	Yes	No	4+5	23	9	14	0	0	N0
68	13.3	No	No	T2a	6.4	N0	0	0	No	No	Yes	No	3+3	15	10	5	0	0	N0
59	131	No	No	T2c	17.5	N1	1	0	Yes	Both	Yes	Yes	4+3	24	13	11	1	1	N1
56	56.1	Yes	No	T3a	5.7	N1	1	1	Yes	No	Yes	Yes	4+3	18	12	6	0	1	N1
70	200.3	No	No	T2b	11.7	N0	0	0	No	No	Yes	No	4+4	16	9	7	0	0	N0
56	100.1	Yes	Both	T3b	30.3	N1	1	1	Yes	Both	Yes	Yes	4+5	28	17	11	1	2	N1
59	36.1	Yes	Right	T3b	48.3	N1	5	4	Yes	Both	Yes	Yes	4+4	33	19	14	6	5	N1
57	10.1	Yes	Both	T3b	14.1	N1	1	1	Yes	Both	Yes	Yes	4+5	15	8	7	1	1	N1
64	40.3	No	No	T2b	27.3	N0	0	0	Focal	No	Yes	Yes	4+4	17	15	2	0	0	N0
50	22.4	Yes	Both	T3b	9.7	N0	0	0	Yes	Both	Yes	Yes	4+4	25	12	13	1	0	N1
66	47.5	Yes	Both	T3b	35.9	N0	0	0	Yes	Both	Yes	Yes	4+3	24	9	15	1	0	N1
66	21.1	No	No	T2c	6.1	N0	0	0	Focal	Left	Yes	Yes	4+5	19	11	8	0	0	N0
70	18.3	No	No	T2c	21.2	N0	0	0	No	No	No	No	4+3	10	3	7	0	0	N0
65	11.1	No	No	T2b	10.1	N0	0	0	Yes	Both	Yes	No	4+4	15	12	3	0	0	N0
										intraprostatic part									
66	5.5	Yes	Both	T3b	17.2	N0	0	0	Yes	Both	Yes	Yes	4+5	27	16	11	0	0	N0
68	24.2	No	No	T2c	3.2	N1	1	1	No	No	No	No	4+4	28	20	8	1	1	N1
66	75.1	Yes	Both	T3b	17.7	N1	2	2	Focal	Both	Yes	Yes	3+4	21	9	12	2	7	N1
70	49.2	Yes	Both	T3b	11.9	N0	0	0	Yes	Both	Yes	No	4+4	21	11	10	0	0	N0
77	43.5	Yes	Both	T3b	19.1	N1	1	1	Yes	No	No	No	4+4	20	14	6	0	0	N0
62	74.8	Yes	Right	T3b	36.2	N0	0	0	Yes	Both	Yes	No	4+4	10	6	4	0	0	N0
69	70.3	No	No	T2c	19.1	N0	0	0	Yes	Both	Yes	No	3+4	34	19	15	0	0	N0

PSA: Prostate-specific antigen; EPE: Extraprostatic extension; SVI: Seminal vesicle invasion; PNI: Perineural invasion; LVI: Lymphovascular invasion; SUV: Standard uptake value; PSMA: Prostatic-specific membrane antigen; PET: Positron emission tomography

**Table 4: Prostatic-specific membrane antigen positron emission tomography-computed tomography detectability for lymph node metastasis per patient basis in comparison to histopathology**

	Histopathology		Total	P	$\kappa$
	Negative (%)	Positive (%)			
PSMA PET-CT					
Negative	13 (56.52)	2 (8.70)	15 (65.22)	0.001	0.721
Positive	1 (4.35)	7 (30.43)	8 (34.78)		
Total	14 (60.87)	9 (39.13)	23 (100.00)		

PET-CT: Positron emission tomography-computed tomography; PSMA: Prostatic-specific membrane antigen

**Table 5: Prostatic-specific membrane antigen positron emission tomography-computed tomography detectability for lymph node metastasis per lymph node basis in comparison to histopathology**

	Histopathology		Total	P	$\kappa$
	Negative (%)	Positive (%)			
PSMA PET-CT					
Negative	434 (92.54)	11 (2.35)	445 (94.88)	<0.0001	0.734
Positive	3 (0.64)	21 (4.48)	24 (5.12)		
Total	437 (93.18)	32 (6.82)	469 (100.00)		

PET-CT: Positron emission tomography-computed tomography; PSMA: Prostatic-specific membrane antigen

**Table 6: Prostatic-specific membrane antigen positron emission tomography-computed tomography and histopathology tumor stage Kappa agreement and level of significance**

	Histopathology tumor stage				Total (%)	P	$\kappa$
	T2a (%)	T2c (%)	T3a (%)	T3b (%)			
PSMA PET-CT (tumor stage)							
T2a	0	1 (4.35)	1 (4.35)	0	2 (8.70)	0.011	0.277
T2b	0	1 (4.35)	1 (4.35)	1 (4.35)	3 (13.04)		
T2c	1 (4.35)	1 (4.35)	1 (4.35)	3 (13.04)	6 (26.09)		
T3a	0	0	1 (4.35)	0	1 (4.35)		
T3b	0	0	1 (4.35)	10 (43.48)	11 (47.83)		
Total	1 (4.35)	3 (13.04)	5 (21.74)	14 (60.87)	23 (100.00)		

PET-CT: Positron emission tomography-computed tomography; PSMA: Prostatic-specific membrane antigen

and prostate SUV<sub>max</sub>) for true-positive lymph node, presence of LVI ( $P = 0.007$ ) and lesser age ( $P = 0.017$ ) were significant risk factors with odds ratio of 29.333 and 0.696, respectively. An inverse relationship with age and lymph node positivity appeared to be due to low number and more positivity of patients in younger age group. On multivariate regression after adjusting for confounding, none of the variables were found to be significant independent risk factor of a true-positive lymph node.

In Gleason score 7 subcategory (7a: 3 + 4, 7b: 4 + 3) analysis, we did not find statistically significant difference ( $P > 0.05$ ) for PSA, PNI, LVI, EPE, SVI, pathological T stage, pathological N stage, and prostate SUV. Gleason score 9 subcategory analysis was not done because in our 23 patients' group, we had only Gleason 9a (4 + 5) subcategory. Prostate SUV showed no correlation with Gleason score ( $r_s = 0.02$ ,  $P = 0.928$ ) and a weak positive correlation with PSA ( $r_s = 0.353$ ,  $P = 0.098$ ). No statistically significant ( $P > 0.05$ ) difference was seen in prostate SUV with PNI, LVI, EPE, SVI, and pathological T and N stage status.

## DISCUSSION

PCa is the second most common cause of cancer and the sixth leading cause of cancer death among men worldwide.<sup>[23]</sup> Although the incidence of PCa in India is lower than that of the Western countries, an increasing trend is seen in metro cities and reached at 2<sup>nd</sup> position in Delhi.<sup>[24]</sup> Risk stratification is the important factor for deciding the further course of management following diagnosis. Currently, this is based on various clinical and histopathological factors and predictive mathematical models. The commonly used variables are PSA, Gleason score, and clinical T stage to divide patients into now practiced three risk categories of low, intermediate, and high risk.<sup>[20,25-28]</sup> We analyzed our staging PSMA PET-CT data by standard and proposed nonstandard three risk categories by taking in account single, two, and three variables in a group. PSMA PET-CT identified an increased incidence of lymph node and distant metastasis with increase in risk categories with statistically significant results. Using standard risk stratification categories, all our patients were of either intermediate (60.82%) or

high (39.18%) risk. PSMA PET-CT helped in prognostication by detection of lymph node and distant metastasis in this group and also directed appropriate management. In our proposed nonstandard risk category based on single variable, <10% patients belonged to low-risk group, with 10%–30% chance of detecting lymph node and metastasis with PSMA PET-CT. However, its precise role in low-risk category needs to be elucidated in a large series of such patients. It is common to see that normally patients with diagnosed PCa usually present with two variables (PSA and Gleason score), and with our results showing a chance of lymph node or distant metastasis even in low-risk category based on one variable, it assumes further importance that the PSMA PET-CT has an edge over conventional modalities during staging of PCa. We found an average 53.78% and 76.47% chance of lymph node/metastasis detection in intermediate- and high-risk categories, respectively, by PSMA PET-CT in two risk variables' group (PSA + Gleason) as well.

Hematogenous metastasis is an important determinant of prognosis and planning treatment in PCa.<sup>[29,30]</sup> An autopsy study of 1589 PCa patients by Bubendorf *et al.*<sup>[31]</sup> showed hematogenous metastases in 35% of patients with most frequent involvement being bone (90%), lung (46%), liver (25%), pleura (21%), and adrenals (13%). In our study, we have 44.33% of patients with hematogenous spread ( $M_{1b} + M_{1c}$ ) during initial presentation. The bone has been a more common (67.31%) site followed by soft tissue (15.38%). Extrapelvic lymph node metastasis is another important factor in decision-making; however, its presence is commonly underestimated with conventional staging methods.<sup>[32-35]</sup> In our study, we found that 17.31% of patients had retroperitoneal lymph node metastasis without evidence of hematogenous spread ( $M_{1a}$ ). In addition, PSMA PET-CT showed incremental value in the detection of inguinal and mediastinal lymph node metastasis, contrasting it from conventional methods.

Currently, BS is recommended in patients with a high risk of metastasis according to many current guidelines.<sup>[36-38]</sup> This is due to the fact that bone is the most common site of metastasis and sclerotic lesion is the most common type. However, it is a well-known fact that BS is nonspecific and many a times it is hard to differentiate between degenerative bone disease and bone metastasis, hence frequently requiring additional imaging modality for characterization.<sup>[39]</sup> In our study, we noticed that only 57.41% of patients with bone metastasis had pure sclerotic lesions. Mixed (33.33%), marrow (7.14%), and lytic (2.3%) types of lesions constitute the rest and thus may lead to underestimation of bony disease burden by BS alone. A recent retrospective study by Pyka *et al.* comparing BS and PSMA PET-CT suggested similar findings.<sup>[40]</sup>

Regional MRI is considered to be an essential imaging modality for planning surgical management.<sup>[41]</sup> It can differentiate and characterize different T stages and can evaluate ECE, involvement of neurovascular bundle, SVI, and invasion of adjacent structures where surgical intervention may not be indicated.<sup>[42]</sup> Porcaro *et al.* reported sensitivity and specificity of 78%, 96% and 88%, 98%, respectively, for preoperative endorectal coil MRI for evaluating ECE and SVI<sup>[43]</sup> as compared to 63.16%, 100% and 55%, 100%, respectively, reported in our study. This was however not statistically significant ( $P = 0.371, 0.760$  and  $0.362, 0.630$ , respectively). PSMA PET-CT was unable to detect 4/5 focal capsule invasion on histopathology and this appeared to be the main reason for lower sensitivity for ECE. This was likely to be due to technical limitation of PET and the surrounding high tracer activity in prostate. For low SVI sensitivity of PET, unilateral or intraprostatic part of SVI involvement was the reason identified in our study.

MRI has a limitation for lymph node evaluation with low sensitivity (27.27%) though the specificity remained high (98.47%).<sup>[44]</sup> That was due to a threshold of 1 cm in the short axis for the oval lymph node and 0.8 cm for the round lymph node as the recommended criteria for morphological imaging. However, 70% of metastatic lymph nodes can be subcentimeter in size.<sup>[45]</sup> In our study, PSMA PET-CT has a better sensitivity (65.62%) and specificity (99.31%) per lymph node basis, which was comparable to literature.<sup>[46,47]</sup> On further analysis of false-negative lymph nodes on PSMA PET-CT, we found that all lymph nodes were subcentimeter in size, and the largest size of lymph node and metastasis missed was 0.7 cm and 0.3 cm, respectively. Even with this limitation of PSMA PET-CT regarding the detection of small sub-cm lymph node, still it has an edge over the current modalities. Our in-press article comparing PSMA PET-CT and MRI for N staging in high-risk PCa patients suggested statistically significant better sensitivity and specificity overall and 55% sensitivity for sub-cm lymph node.<sup>[48]</sup>

There were few limitations in this study. There was no real comparison with BS which is the current standard imaging modality. Although it is predicted that PSMA PET-CT will outscore BS in the evaluation of bone metastasis, we suggest that this needs to be evaluated in a large patient cohort. Another limitation was that the histopathology of distant metastatic sites was not available. This was due to either presence of many metastatic sites or locally advanced inoperable disease. We have seen the metastatic potential of low-risk patients and as mentioned previously it needs to be validated in a large study and this should be one of the focused researches in PSMA PET-CT in the future. For initial

risk stratification, PSMA PET-CT was found to be promising; however, risk stratification for treatment outcome and survival needs long-term studies and a direct comparison with the currently available predictive models.

## CONCLUSION

PSMA PET-CT appeared to be promising for initial risk stratifications and showed statistically significantly increased risk of lymph node and distant metastasis with increase in risk categories. For N stage, it showed promising result with reasonable correct estimation and substantial agreement with histopathology. However, in T stage, it has the propensity to underestimate although it was not statistically significant. We conclude that PSMA PET-CT should be used for staging and initial risk stratification of PCa as first-stop-shop imaging with the addition of regional MRI in potentially surgically resectable cases.

## Financial support and sponsorship

Nil.

## Conflicts of interest

There are no conflicts of interest.

## REFERENCES

- Hövels AM, Heesakkers RA, Adang EM, Jager GJ, Strum S, Hoogeveen YL, *et al.* The diagnostic accuracy of CT and MRI in the staging of pelvic lymph nodes in patients with prostate cancer: A meta-analysis. *Clin Radiol* 2008;63:387-95.
- Jacobson AF, Fogelman I. Bone scanning in clinical oncology: Does it have a future? *Eur J Nucl Med* 1998;25:1219-23.
- Schirmeister H, Glattig G, Hetzel J, Nüssle K, Arslanemir C, Buck AK, *et al.* Prospective evaluation of the clinical value of planar bone scans, SPECT, and (18F)-labeled NaF PET in newly diagnosed lung cancer. *J Nucl Med* 2001;42:1800-4.
- Partin AW, Mangold LA, Lamm DM, Walsh PC, Epstein JI, Pearson JD, *et al.* Contemporary update of prostate cancer staging nomograms (Partin tables) for the new millennium. *Urology* 2001;58:843-8.
- Kattan MW, Potters L, Blasko JC, Beyer DC, Fearn P, Cavanagh W, *et al.* Pretreatment nomogram for predicting freedom from recurrence after permanent prostate brachytherapy in prostate cancer. *Urology* 2001;58:393-9.
- Cagiannos I, Karakiewicz P, Eastham JA, Ohori M, Rabbani F, Gerigk C, *et al.* A preoperative nomogram identifying decreased risk of positive pelvic lymph nodes in patients with prostate cancer. *J Urol* 2003;170:1798-803.
- Augustin H, Eggert T, Wenske S, Karakiewicz PI, Palisaar J, Daghofer F, *et al.* Comparison of accuracy between the Partin tables of 1997 and 2001 to predict final pathological stage in clinically localized prostate cancer. *J Urol* 2004;171:177-81.
- Eifler JB, Feng Z, Lin BM, Partin MT, Humphreys EB, Han M, *et al.* An updated prostate cancer staging nomogram (Partin tables) based on cases from 2006 to 2011. *BJU Int* 2013;111:22-9.
- Rodrigues G, Warde P, Pickles T, Crook J, Brundage M, Souhami L, *et al.* Pre-treatment risk stratification of prostate cancer patients: A critical review. *Can Urol Assoc J* 2012;6:121-7.
- Green DA, Osterberg EC, Xylinas E, Rink M, Karakiewicz PI, Scherr DS, *et al.* Predictive tools for prostate cancer staging, treatment response and outcomes. *Arch Esp Urol* 2012;65:787-807.
- Conti M. New prospects for PET in prostate cancer imaging: A physicist's viewpoint. *EJNMMI Phys* 2014;1:11.
- Wright GL Jr., Haley C, Beckett ML, Schellhammer PF. Expression of prostate-specific membrane antigen in normal, benign, and malignant prostate tissues. *Urol Oncol* 1995;1:18-28.
- Afshar-Oromieh A, Avtzi E, Giesel FL, Holland-Letz T, Linhart HG, Eder M, *et al.* The diagnostic value of PET/CT imaging with the (68)Ga-labelled PSMA ligand HBED-CC in the diagnosis of recurrent prostate cancer. *Eur J Nucl Med Mol Imaging* 2015;42:197-209.
- Eiber M, Maurer T, Souvatzoglou M, Beer AJ, Ruffani A, Haller B, *et al.* Evaluation of hybrid 68Ga-PSMA ligand PET/CT in 248 patients with biochemical recurrence after radical prostatectomy. *J Nucl Med* 2015;56:668-74.
- Perera M, Papa N, Christidis D, Wetherell D, Hofman MS, Murphy DG, *et al.* Sensitivity, specificity, and predictors of positive 68Ga-prostate-specific membrane antigen positron emission tomography in advanced prostate cancer: A systematic review and meta-analysis. *Eur Urol* 2016;70:926-37.
- Herlemann A, Wenter V, Kretschmer A, Thierfelder KM, Bartenstein P, Faber C, *et al.* 68Ga-PSMA positron emission tomography/computed tomography provides accurate staging of lymph node regions prior to lymph node dissection in patients with prostate cancer. *Eur Urol* 2016;70:553-7.
- Uprimny C, Kroiss AS, Decristoforo C, Fritz J, von Guggenberg E, Kendler D, *et al.* 68Ga-PSMA-11 PET/CT in primary staging of prostate cancer: PSA and Gleason score predict the intensity of tracer accumulation in the primary tumour. *Eur J Nucl Med Mol Imaging* 2017;44:941-9.
- Zang S, Shao G, Cui C, Li TN, Huang Y, Yao X, *et al.* 68Ga-PSMA-11 PET/CT for prostate cancer staging and risk stratification in Chinese patients. *Oncotarget* 2017;8:12247-58.
- Edge SB, Byrd DR, Compton CC, Fritz AG, Greene FL, Trotti A. *AJCC cancer staging manual*. 7<sup>th</sup> edition. France: Springer; 2010. p. 457-68.
- Mohler J, Bahnson RR, Boston B, Busby JE, D'Amico A, Eastham JA, *et al.* NCCN clinical practice guidelines in oncology: Prostate cancer. *J Natl Compr Canc Netw* 2010;8:162-200.
- Amor-Coarasa A, Schoendorf M, Meckel M, Vallabhajosula S, Babich JW. Comprehensive quality control of the ITG 68Ge/68Ga generator and synthesis of 68Ga-DOTATOC and 68Ga-PSMA-HBED-CC for clinical imaging. *J Nucl Med* 2016;57:1402-5.
- Fendler WP, Eiber M, Beheshti M, Bomanji J, Ceci F, Cho S, *et al.* 68Ga-PSMA PET/CT: Joint EANM and SNMMI procedure guideline for prostate cancer imaging: Version 1.0. *Eur J Nucl Med Mol Imaging*. 2017;44:1014-24.
- Yeole BB. Trends in the prostate cancer incidence in India. *Asian Pac J Cancer Prev* 2008;9:141-4.
- Jain S, Saxena S, Kumar A. Epidemiology of prostate cancer in India. *Meta Gene* 2014;2:596-605.
- Graham J, Baker M, Macbeth F, Titshall V; Guideline Development Group. Diagnosis and treatment of prostate cancer: Summary of NICE guidance. *BMJ* 2008;336:610-2.
- Horwich A, Parker C, Bangma C, Kataja V; ESMO Guidelines Working Group. Prostate cancer: ESMO clinical practice guidelines for diagnosis, treatment and follow-up. *Ann Oncol* 2010;21 Suppl 5:v129-33.
- Thompson I, Thrasher JB, Aus G, Burnett AL, Canby-Hagino ED, Cookson MS, *et al.* Guideline for the management of clinically localized prostate cancer: 2007 update. *J Urol* 2007;177:2106-31.
- Heidenreich A, Aus G, Bolla M, Joniau S, Matveev VB, Schmid HP, *et al.* EAU guidelines on prostate cancer. *Eur Urol* 2008;53:68-80.
- Wong SY, Hynes RO. Lymphatic or hematogenous dissemination: How does a metastatic tumor cell decide? *Cell Cycle* 2006;5:812-7.
- Attard G, Parker C, Eeles RA, Schröder F, Tomlins SA, Tannock I, *et al.*



- Prostate cancer. *Lancet* 2016;387:70-82.
31. Bubendorf L, Schöpfer A, Wagner U, Sauter G, Moch H, Willi N, *et al.* Metastatic patterns of prostate cancer: An autopsy study of 1,589 patients. *Hum Pathol* 2000;31:578-83.
  32. Cai T, Nesi G, Tinacci G, Giubilei G, Gavazzi A, Mondaini N, *et al.* Clinical importance of lymph node density in predicting outcome of prostate cancer patients. *J Surg Res* 2011;167:267-72.
  33. Löppenber B, Dalela D, Karabon P, Sood A, Sammon JD, Meyer CP, *et al.* The impact of local treatment on overall survival in patients with metastatic prostate cancer on diagnosis: A national cancer data base analysis. *Eur Urol* 2017;72:14-9.
  34. O'Shaughnessy MJ, McBride SM, Vargas HA, Touijer KA, Morris MJ, Danila DC, *et al.* A pilot study of a multimodal treatment paradigm to accelerate drug evaluations in early-stage metastatic prostate cancer. *Urology* 2017;102:164-72.
  35. Tosoian JJ, Gorin MA, Ross AE, Pienta KJ, Tran PT, Schaeffer EM, *et al.* Oligometastatic prostate cancer: Definitions, clinical outcomes, and treatment considerations. *Nat Rev Urol* 2017;14:15-25.
  36. Cook GJ, Azad G, Padhani AR. Bone imaging in prostate cancer: The evolving roles of nuclear medicine and radiology. *Clin Transl Imaging* 2016;4:439-47.
  37. Wollin DA, Makarov DV. Guideline of guidelines: Imaging of localized prostate cancer. *BJU Int* 2015;116:526-30.
  38. Heidenreich A, Bastian PJ, Bellmunt J, Bolla M, Joniau S, van der Kwast T, *et al.* EAU guidelines on prostate cancer. Part 1: Screening, diagnosis, and local treatment with curative intent-update 2013. *Eur Urol* 2014;65:124-37.
  39. Messiou C, Cook G, deSouza NM. Imaging metastatic bone disease from carcinoma of the prostate. *Br J Cancer* 2009;101:1225-32.
  40. Pyka T, Okamoto S, Dahlbender M, Tauber R, Retz M, Heck M, *et al.* Comparison of bone scintigraphy and <sup>68</sup>Ga-PSMA PET for skeletal staging in prostate cancer. *Eur J Nucl Med Mol Imaging* 2016;43:2114-21.
  41. Murphy G, Haider M, Ghai S, Sreeharsha B. The expanding role of MRI in prostate cancer. *AJR Am J Roentgenol* 2013;201:1229-38.
  42. Villers A, Lemaitre L, Haffner J, Puech P. Current status of MRI for the diagnosis, staging and prognosis of prostate cancer: Implications for focal therapy and active surveillance. *Curr Opin Urol* 2009;19:274-82.
  43. Porcaro AB, Borsato A, Romano M, Sava T, Ghimenton C, Migliorini F, *et al.* Accuracy of preoperative endo-rectal coil magnetic resonance imaging in detecting clinical under-staging of localized prostate cancer. *World J Urol* 2013;31:1245-51.
  44. Wang L, Hricak H, Kattan MW, Schwartz LH, Eberhardt SC, Chen HN, *et al.* Combined endorectal and phased-array MRI in the prediction of pelvic lymph node metastasis in prostate cancer. *AJR Am J Roentgenol* 2006;186:743-8.
  45. Jager GJ, Barentsz JO, Oosterhof GO, Witjes JA, Ruijs SJ. Pelvic adenopathy in prostatic and urinary bladder carcinoma: MR imaging with a three-dimensional T1-weighted magnetization-prepared-rapid gradient-echo sequence. *AJR Am J Roentgenol* 1996;167:1503-7.
  46. van Leeuwen PJ, Emmett L, Ho B, Delprado W, Ting F, Nguyen Q, *et al.* Prospective evaluation of <sup>68</sup>Gallium-prostate-specific membrane antigen positron emission tomography/computed tomography for preoperative lymph node staging in prostate cancer. *BJU Int* 2017;119:209-15.
  47. Maurer T, Gschwend JE, Rauscher I, Souvatzoglou M, Haller B, Weirich G, *et al.* Diagnostic efficacy of (68)Gallium-PSMA positron emission tomography compared to conventional imaging for lymph node staging of 130 consecutive patients with intermediate to high risk prostate cancer. *J Urol* 2016;195:1436-43.
  48. Gupta M, Choudhury PS, Hazarika D, Rawal S. A comparative study of <sup>68</sup>Gallium-prostate specific membrane antigen positron emission tomography-computed tomography and magnetic resonance imaging for lymph node staging in high risk prostate cancer patients: An initial experience. *World J Nucl Med* 2017;16:186-91.